# Validation of High Displacement Piezoelectric Actuator Finite Element Models

Barmac Taleghani*
Army Research Laboratory
Vehicle Technology Directorate
NASA Langley Research Center
Hampton, VA

## ABSTRACT

The paper presents the results obtained by using NASTRAN® and ANSYS® finite element codes to predict doming of the THUNDER piezoelectric actuators during the manufacturing process and subsequent straining due to an applied input voltage. To effectively use such devices in engineering applications, modeling and characterization are essential. Length, width, dome height, and thickness are important parameters for users of such devices. Therefore, finite element models were used to assess the effects of these parameters. NASTRAN® and ANSYS® used different methods for modeling piezoelectric effects. In NASTRAN®, a thermal analogy was used to represent voltage at nodes as equivalent temperatures, while ANSYS® processed the voltage directly using piezoelectric finite elements. The results of finite element models were validated by using the experimental results.

Keywords: NASTRAN®, ANSYS®, finite element, THUNDER, piezoelectric, actuator

## 1. INTRODUCTION

THUNDER [1] (**TH**in Layer **Un**imorph Ferroelectric **D**riv**ER**), shown in Figure 1, is a high displacement piezoelectric actuator (developed at NASA Langley Research Center) that provides significantly larger displacements than those available previously in other piezoelectric actuators. THUNDER is a composite laminate consisting of a metal substrate (e.g., stainless steel) LaRC-SI™, PZT, LaRC-SI™, and aluminum (Figure 2) that is formed when the composite laminate is heated to a temperature beyond the glass transition temperature of LaRC-SI™ and cooled to room temperature. During cooling, the different coefficients of thermal expansion (CTE) lead to a domed shape. The dome shape results in a component of stress being out of plane, and that out-of-plane stress results in increase of the dynamic deflection. The design has made this type of actuator attractive for applications such as motors, speakers, and air pumps.

Figure 1. THUNDER actuator

To date, there have been limited modeling efforts to understand the THUNDER dynamic behavior [1, 2]. The major parameters that determine the behavior of the THUNDER actuators are the type of PZT used, the physical properties of constituent layers, the uniformity of the LaRC-SI™ layer, the autoclave temperature and pressure profile, and the thickness of the piezo ceramic.

* b.k.taleghani@larc.nasa.gov; Telephone: +1-757-864 8499; Fax: +1 757-864 8808

Recently, a nonlinear NASTRAN® [3] (Version 70.5) model was developed to capture the influence of the above-cited parameters and to analytically predict doming of the actuator during the manufacturing process and due to applied voltage. A simple approach was used in which temperature-induced expansion simulated voltage actuation, as described by Babuska et al. [4]. Since then, various finite element codes (e.g. ANSYS®), which have coupled field capabilities, have been investigated by the author. The objective of this research is to evaluate the results of NASTRAN® and ANSYS® [5] (Version 5.6) finite element modeling capability for piezoelectric actuators and compare the analyses with experimental data.

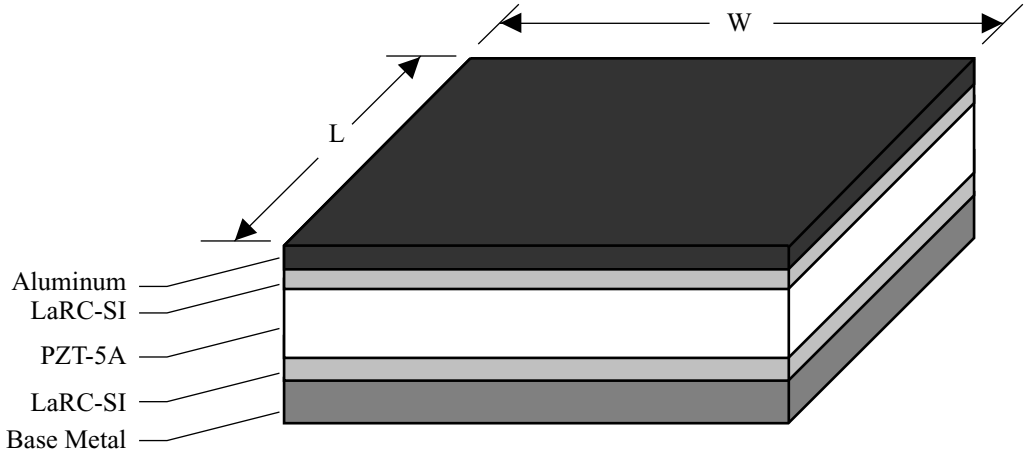


Figure 2. THUNDER composite laminate

## 2. MODELING APPROACHES

### 2.1 NASTRAN® Approach

The NASTRAN® linear modeling approach assumes that at a glass transition temperature of LaRC-SI™ (assumed to be 250°C), all layers are bonded. The bonding constrains all layers to move together while the specimen is cooled to room temperature (25°C). The model only accounts for the portion of the process in which the device is cooled from 250°C to room temperature, thus generating thermal stress due to differing CTE's in the layers. The analysis subsequently is divided into two parts, as described in ref. 2. The first part is the fabrication cooling process where the initial doming occurs. The second part is the straining of the device due to applied voltage where the voltage is represented by an equivalent temperature.

### 2.2 ANSYS® Approach

The ANSYS® linear modeling approach uses a coupled field capability, which allows for direct application of the voltage to the PZT layers.

The constitutive equations for piezoelectricity from reference [5] are

$$\{T\} = [c]\{S\} - [e]\{E\} \quad (1)$$

$$\{D\} = [e]^T\{S\} + [\varepsilon]\{E\} \quad (2)$$

where

T represents 6 components of stress,

c diagonal matrix is the system stiffness matrix,
S represents 6 components of strain,
e is the piezoelectric matrix,
E represents the 3 components of the electric field,
D represents the 3 components of the electric flux density, and
ε is the dielectric matrix relating the electric field to electric flux density.

The material properties which populate the matrices in eqs. (1) and (2) are not easily measured directly. However, the properties in the inverses of the matrices are readily available; therefore, an alternate form of the equations is introduced

$$\{S\} = [c^E]\{T\} + [d]\{E\} \quad (3)$$

$$\{D\} = [d]^T\{T\} + [P]\{E\} \quad (4)$$

where

$c^E$ diagonal is the compliance matrix for the elastic system,
d is the dielectric matrix which related electric field to strain, and
P is the diagonal permittivity matrix

Comparing eqs. (1) and (2) with (3) and (4) gives

$$[c] = [c^E]^{-1} \quad (5)$$

$$[e] = [c^E]^{-1}[d] \quad (6)$$

then

$$[e]^T = [d]^T [c^E]^{-1} \quad (7)$$

$$[\varepsilon] = [P] - [d]^T [c^E]^{-1}[d] \quad (8)$$

In the above analysis, the material properties for all the layers, excluding the PZT layer, are isotropic. The modulus of elasticity, the Poisson ratio, and the coefficient of thermal expansion are directly input into the matrices $[c^E]$, [d], and [P] and equations (5) - (8) used to generate the matrices in equations (1) and (2). As an aid to ANSYS® users, the PIEZMAT macro has been created that will convert the manufacturer's data into ANSYS® form.

## 3. TEST SPECIMENS

To assess the NASTRAN® and ANSYS® finite element models, four groups of specimens were fabricated and tested. The material properties and the composition for the above comparison are shown in Table 1 (a) and (b) and Table 2.

(a) Properties of specimens (all groups)

| Layers | Material | Thickness (in.) | Modulus of Elasticity (E) (psi) $\times 10^6$ | Poisson's Ratio | Coefficient of Thermal Expansion (CTE) $10^{-6}/^0C$ |
|---|---|---|---|---|---|
| 1 (Top Layer) | Aluminum | 0.001 | 10 | 0.33 | 24.0 |
| 2 | LaRC-SI™ | 0.001 | 0.58 | 0.45 | 46 |
| 3 | PZT 5A | 0.0068 | 9.8 | 0.31 | 1.5 |
| 4 | LaRC-SI™ | 0.001 | 0.58 | 0.45 | 46 |
| 5 (Bottom layer) | Stainless Steel | | 38 | 0.33 | 17.3 |

(b) PZT-5A Material Properties [6]

| | |
|---|---|
| $C^E_{11}$ | 1.13E-7 $in^2$/lbf |
| $C^E_{33}$ | 1.29E-7 $in^2$/lbf |
| $C^E_{44}$ | 3.27E-7 $in^2$/lbf |
| $C^E_{12}$ | -3.92E-8 $in^2$/lbf |
| $C^E_{13}$ | -4.92E-8 $in^2$/lbf |
| $d_{31}$ | -6.7E-9 in/Volt |
| $d_{33}$ | 1.47E-8 in/Volt |
| $d_{15}$ | 2.30E-8 in/Volt |
| $P_{33}$ | 3.82E-10 Farads/in. |
| $P_{11}$ | 3.88E-10 Farads/in. |

There are four groups of specimens (see Table 2). The groups are based on two sets of planform dimensions ($1 \times 1$ inch and $1 \times 2$ inch) and two sets of base metal thickness (3 mil and 5 mil).

Definition of groups

| Thickness | Dimension L × W<br>1 × 1 | Dimension L × W<br>2 × 1 |
|---|---|---|
| 3 mil | Group 1 | Group 3 |
| 5 mil | Group 2 | Group 4 |

Table 2. Composition of test specimens

For testing purposes, the wafers were mounted by using an adhesive tape to constrain lateral movement but to allow vertical displacement. This mounting technique can introduce variability in the displacement data which future improvements should alleviate.

## 4. FINITE ELEMENT MODEL DESCRIPTIONS

The models were developed and meshed by using I-DEAS® [7] Master Series (Version 6.0). Creating all the layers and stacking them developed the 3D geometry model. In all models, only a quarter of the actuator was modeled by using symmetry.

### 4.1 NASTRAN® Model

The NASTRAN® linear finite element models used CHEXA 8 solid elements. Free-free boundary conditions were used for these analyses. The smallest and the largest aspect ratios, which were measured in length and thickness for the solids were 1:12.5 and 1:5, respectively. The model for group 1 consisted of 16,810 nodes, 11,200 solid elements, 50,000 degrees of freedom, and 3362 multipoint constraints. The model for group 2 consisted of 18,499 nodes, 12,800 elements, 55,000 degrees of freedom, and 3362 multipoint constraints. Group 3 included 18,360 nodes, 12,250 elements, 55,000 degrees of freedom, and 3672 multipoint constraints. Group 4 used 3672 multipoint constraints, 20,196 nodes, 14,000 elements, and 60,000 degrees of freedom. Since solid elements were used in NASTRAN®, it was necessary to contain the applied temperature, which represented the voltage to the nodes belonging to the PZT layer. This containment was achieved by creating coincident nodes between the PZT and the LaRC-Si™ layers. The coincident nodes were then attached by using multipoint constraints.

### 4.2 ANSYS® Model

The finite element models from IDEAS® were imported into ANSYS®. Since ANSYS® does not support external multipoint constraints from other codes, all the coincident nodes, as well as the multipoint constraints were removed. Solid 5 and solid 45 elements were used to model all layers. The number of nodes for groups 1 and 2 were 13,448 and 15,129, respectively. Group 3 and 4 had 14,688 and 16,524 nodes, respectively. All specimens included the same number of elements as the NASTRAN® models.

## 5. RESULTS

NASTRAN® and ANSYS® finite element results were compared to experimental results. Due to the variability in the test data, average values for all measured dome heights are presented. Dome heights due to the manufacturing process and voltage inputs were compared for four groups. The comparison with experimental data for displacements due to input voltages and the dome heights are shown in figures 3, 4, 5, and 6 and in Table 3.

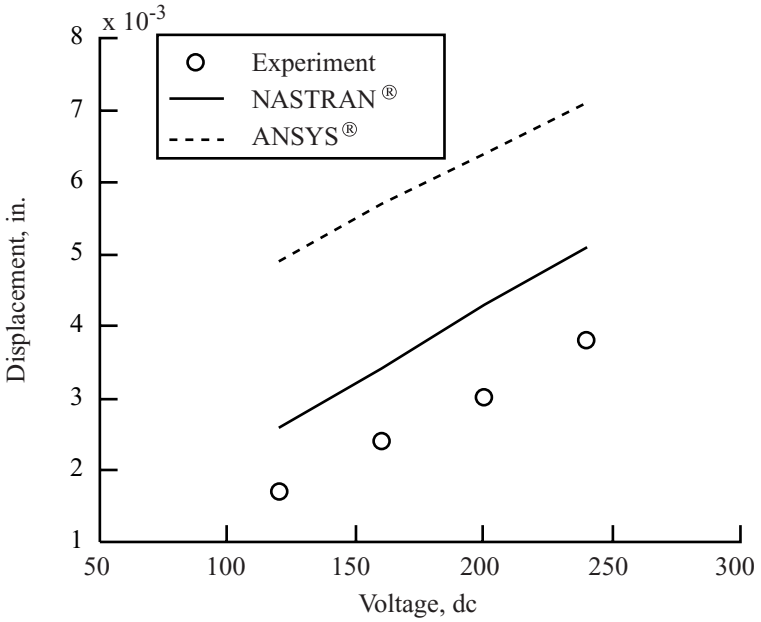


Figure 3. Comparison between finite element models and experimental results for group 1

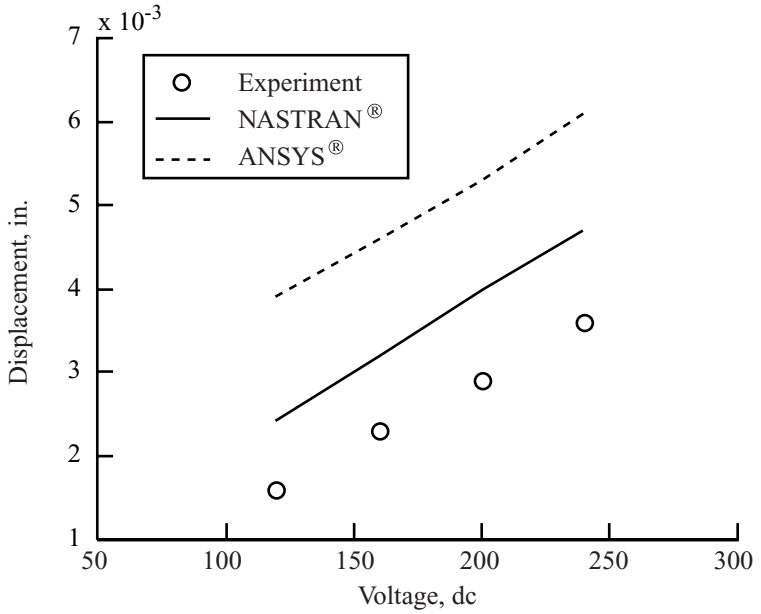


Figure 4. Comparison between finite element models and experimental results for group 2

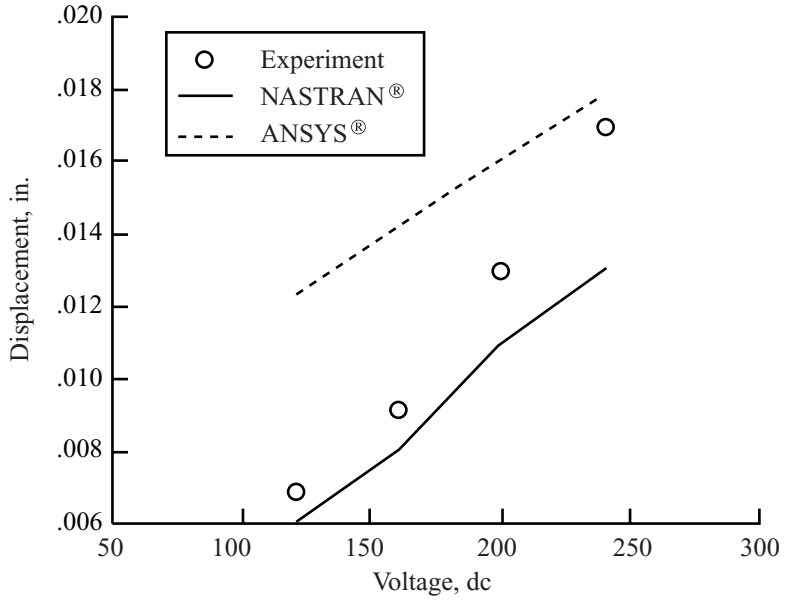


Figure 5. Comparison between finite element models and experimental results for group 3

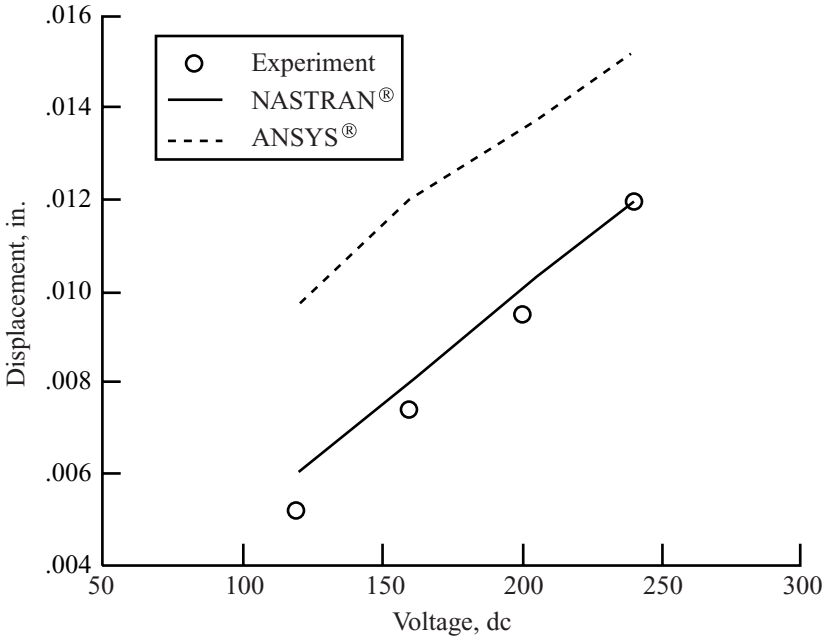


Figure 6. Comparison between finite element models and experimental results for group 4

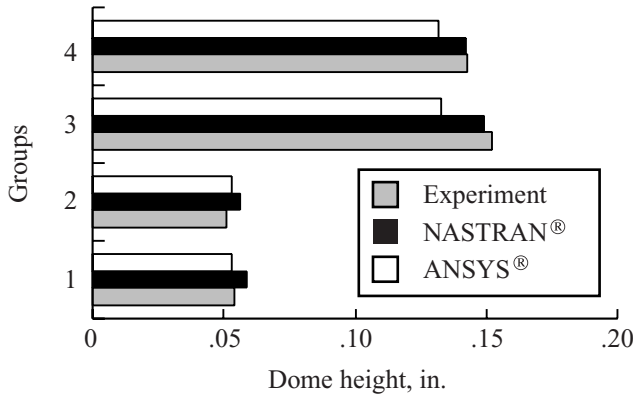


Table 3. Comparison of dome heights due to manufacturing process

From Table 3, we see that all the dome heights due to the manufacturing process for both models agree very well with the experimental results. The difference for NASTRAN® and the experimental data was between 1% to 10%. For ANSYS®, the differences were 2% to 12%.

The THUNDER wafers were driven at 1 Hz at voltages of 120, 160, 200, and 240 volts peak-to-peak (Vp-p) with a 0-volt offset. A fiber optic sensor was placed above the wafer to measure the vertical displacement. The range of the sensor was 50 mils with micro-inch resolution at 1 Hz.

In figures 3, 4, 5, and 6, it is apparent that NASTRAN® follows the trend of experimental results. NASTRAN® has overpredicted the displacements for groups 1, 2, and 4. In all figures, NASTRAN® has slightly different slope than the experimental data. Figures 3 and 4 show a large bias between the NASTRAN® and experimental data. For figures 5 and 6, this bias is much less. In figure 5, the NASTRAN® error also increases as the voltage increases, while for figure 6, the error is reduced as the voltage increases. The percent differences for the third and fourth groups ranged between 12% to 24% and 0% to 15%, respectively. For groups 1 and 2, the percent differences were 34% to 53% and 31% to 50%, respectively.

ANSYS® also over predicted the displacements due to input voltages for all groups. In figure 5 ANSYS® shows a shallower slope compared to the experimental data. ANSYS® errors were largest at low voltages for groups 1 and 2. This trend was completely opposite for groups 3 and 4. In figures 3 and 4, ANSYS® errors are smallest as voltage increases. In all figures a bias exists between ANSYS® and experimental results. For groups 1 and 2, the percent differences for ANSYS® and the experimental results ranged between 87% to 188% and 70% to 143%, respectively. Groups 3 and 4 showed a percent difference of 6% to 78% and 27% to 87%, respectively.

A further study was done to see how ANSYS® and NASTRAN® compare when there is only voltage applied to a structure that is free of initial stresses, i.e., no initial doming. Figure 7 shows the comparison made for group 2. The NASTRAN® and ANSYS® finite element models show good correlation with experimental results and with each other. Both models follow the trend of the experimental results.

The experimental results depicted in ref. 2, as well as here, show a linear behavior. However, nonlinear analysis predicted displacements due to input voltage with much higher accuracy than the linear models. This apparent contradiction could be the result of choosing a narrow range of voltages for the analyses. In such a narrow range, the effects of nonlinearities are not readily observed.

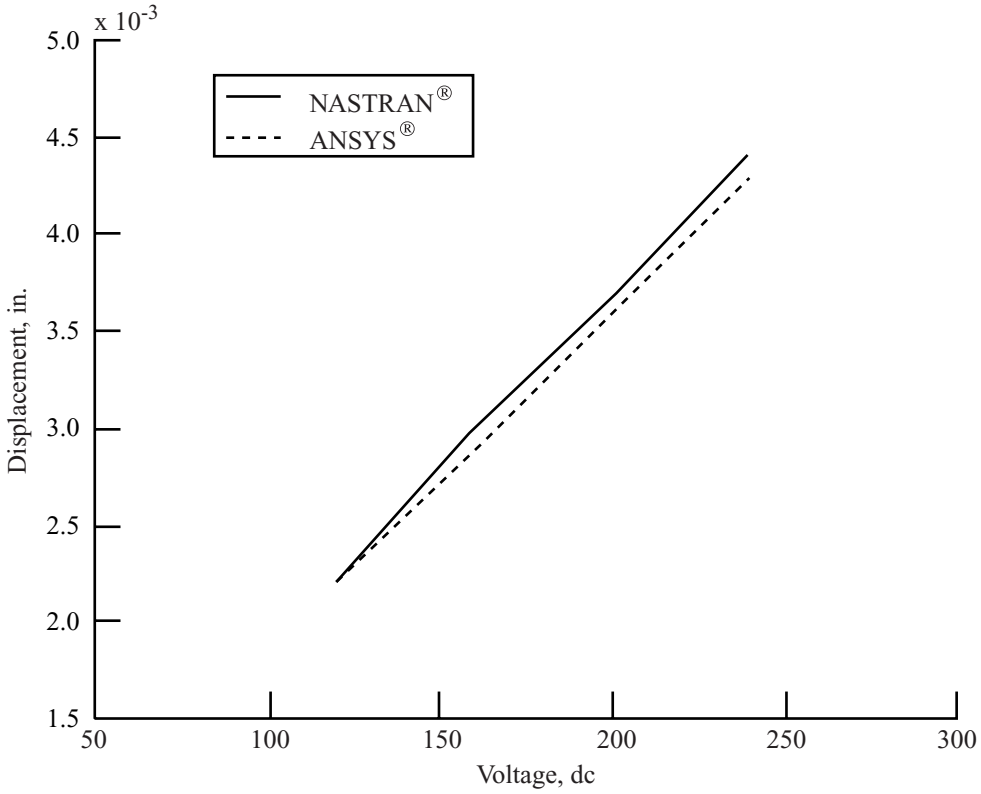


Figure 7. Comparison between the two finite element models and experimental results for group 2 without the manufacturing process

## 6. CONCLUSION

Two linear finite element models, one using a simple thermal analogy (NASTRAN®) and the other using piezoelectric capability (ANSYS®), were developed and evaluated for predicting deformations of the THUNDER piezoelectric actuator concept. Experimental results were compared with each of the finite element results. Both NASTRAN® and ANSYS® showed very good agreement with test data for dome heights due to the manufacturing process. The comparison of dome heights due to the manufacturing process showed differences between 1% to 10% for NASTRAN® and 2% to 12% for ANSYS®. The comparison of displacements due to input voltages (with experimental results) showed differences of 0% to 53% for NASTRAN® and 6% to 188% for ANSYS®. This study suggests that both NASTRAN® and ANSYS® show promise for predicting the dome heights and displacements due to the manufacturing process, as well as induced voltages of THUNDER devices. However, due to geometric nonlinearity, which exists in this type of actuator, a nonlinear analysis is generally needed to predict deformations with high levels of accuracy.

## ACKNOWLEDGEMENTS

The author thanks Michael Lindell and Dr. William F. Hunter, Engineering Analysis Branch, Tommy Jordan, Data Systems and Instrument Support Branch, Joycelyn Harrison, Composite and Polymers Branch, Robert Fox, Microelectronics and Technical Support Section at NASA Langley Research Center, and Zoubeida Ounaice, a National Research Council associate in residence in the Composite and Polymers Branch, for their assistance with finite element modeling as well as fabrication and testing of specimens.

## REFERENCES


1. R. G. Bryant, K. M. Mossi, G. V. Selby, "*Thin-layer Composite Unimorph ferroelectric driver and sensor properties*." Materials Letters, August 1997.

2. B.K. Taleghani, J.F. Campbell "Non-Linear finite element modeling of THUNDER piezoelectric actuators', *Smart Structures and Materials. Smart Structures and Integrated Systems*, vol. 3668, Newport Beach 1999, pp. 555-566.

3. J. P. Caffrey and J. M. Lee, MSC / NASTRAN® Handbook for Non-Linear analysis, The MacNeil Schwendler Corporation, 1994.

4. V. Babuska and B. D. Freed, "Finite Element Modeling of Composite Piezoelectric Structures with MSC/NASTRAN®." *Proceedings, SPIE Smart Structures and Materials*. Paper 3041-60 March 1997.

5. Kohnke, P., ANSYS Theory Reference, Release 5.6, ANSYS Inc., 1999

6. Morgan Matroc Inc., Piezoceramic Databook. Morgan Matroc Inc., Electronic Division.

7. I-DEAS™ Simulation User's Guide, Vol. I & II, Structural Dynamics Research Corporation, 1996.